THERMODYNAMIC ANALYSIS OF EXHAUST HEAT RECOVERY OF MARINE ICE USING ORGANIC RANKINE CYCLE

Shucheng WANG[1], Xinna CHEN[1], Hongwei LI[1], Zhongguang FU[2], Zhicheng HAN[3]*

[*1] School of Energy Power and Engineering, Northeast China Electric Power University, Jilin 132002, China

[2] School of Energy, Power and Mechanical Engineering, North China Electric Power University, Beijing 102206, China

[3] ENFI Institute, China ENFI Engineering Technology Co., Ltd. Beijing 100036, China

[*] Corresponding author; E-mail: zhicheng-han@163.com

The use of organic Rankine cycle power systems for waste heat recovery on marine internal combustion engines can help to mitigate the greenhouse gases and reduce the fuel consumption of the marine engine. In this paper, the internal combustion engine combined with an organic Rankine cycle system was developed to analyze the performance of waste heat recovery from the exhaust gas of a heavy-duty marine diesel engine via five selected working fluids with low global warming potential and ozone depletion potential. The net output power and thermal efficiency for each of the selected working fluids were obtained. Results indicate that the working fluids of butane have the best performance among the selected working fluids with the power efficiency of the organic Rankine cycle subsystem of 12.27% under the power load of 100%. For the overall proposed system, the maximum net power output is 1048kW and the power efficiency is 36.47%. Besides, the total thermal efficiency of the proposed system was 67.94% when considering the recovered waste energy from jacket water.

Key words*: Organic Rankine cycle, Marine diesel engine, Waste heat recovery, Thermodynamic analysis*

1. Introduction

Due to increasing worldwide concerns about the environmental problems caused by fossil fuel consumption and the crises related to the no renewable energy [1, 2]. Maximizing energy saving and improving the efficiency of the energy system have been developed as an economic and environmentally friendly alternative.

Of all the fossil fuels consumed, 60–70% are consumed by internal combustion engines (ICEs) [3]. While a need emerged to enhance ICEs efficiency using waste heat recovery for energy utilization. To reduce the pollution caused by the ship and improve the power system efficiency, the International Marine Organization (IMO) suggested that the total CO_2 emissions of the shipping sector should be reduced to 50% by 2050 (based 2018), which means designing and optimizing waste heat recovery (WHR) systems that recover waste heat energy and reduce the level of emissions at the same time have become attractive investments for ship owners [4-7].

Researchers indicated that the conversion of engine waste heat to useful energy was one promising mechanism to increase the thermal efficiency of marine diesel engines [8]. The efficiency of ICE is about 35% while much of the rest of the energy input is wasted in the surrounding via the exhaust gas. Therefore, WHR from the exhaust gas is known as one of the best energy-saving methods due to its high mass flow rate and high temperature.

In recent years many technologies and operating strategies have been proposed and adopted to improve the overall system efficiency and reduce emissions. Growing numbers of works on the steam Rankine cycle, ORC, Kalina cycle, and CO_2-based power cycles have been witnessed on board ships. Toro and Lior [9] compared the thermodynamic performance and economic benefit of solar-driven Brayton, Rankine and Stirling cycles. The results revealed that the Brayton cycle has significant advantages in thermodynamic performance, while the Stirling cycle has higher efficiency in economic benefit. Lion et al.[10] simulated a marine diesel engine and validated it by the experimental data. The results show that it is possible to develop marine Diesel engines which exhibit fuel consumption levels comparable to those of Tier-II operations and obtain the maximum net power output by recovering the waste heat of exhaust gas. Liu et al.[11] proposed a waste heat recovery system to reduce the fuel consumption and pollutant emission of the marine engines via converting the waste heat of exhaust gas and jacked cooling water into mechanical energy. They indicated that the efficiency of the marine engine could be improved by 4.42%. Mohammed et al.[12] recovered the waste heat of the marine engine from supercritical ORC. Results show that it has a satisfactory performance with respect to the saving in specific fuel consumption by using the supercritical ORC with R124a. Song et al. [13] analyzed (conducted) the performance of an ORC waste heat recovery system for a marine diesel engine. Simulation results reveal that the optimized system is technically feasible and economically attractive. Nawi et al. [8] revealed that conversing the marine diesel engine waste heat with mechanical energy and electrical is a promising way to achieve improvement in thermal systems. Therefore, their research showed that the approximate efficiency of 2.28% and the net power output of 5.1 kW were achieved via the ORC. Ouyang et al. [14] proposed an exergy-based configuration design for a marine cascade waste heat recovery system. Results proved that the proposed cycle configuration has significant thermodynamic performance and economic benefits. And it reflected a good performance of energy saving and emission reduction. Liu et al. [11] proposed a new kind of waste heat recovery system to reduce fuel consumption and pollutant emission. The waste energy is recovered into useful mechanical energy. Results showed that the proposed system improved the thermal efficiency by 4.42%. Mohammed et al. [12] investigated a bulk carrier as a case study to recover wasted heat into power and electricity. Results showed that R134a at a working pressure of 50 bar had a satisfactory performance in saving on specific fuel consumption. The wasted heat of the main engine will decrease by 18%.

The working fluid is evaporated from a saturated liquid to a superheated condition, hence the heat source in the evaporators must be well matched. As a result, the evaporator's output power is higher when the working fluid is less irreversible[15]. Furthermore, the working fluid's chemical and physical qualities have a significant impact on ORC thermal performance and efficiency [16]. Toluene[17], benzene, cyclohex, hexane, ihexane, pentane, R123[18], R245fa[19, 20], R245ca, and R134[19, 21] were all used as working fluids in the ICE-ORC system. Toluene, benzene, cyclohex, hexane, ihexane, and pentane are the most acceptable working fluids for ICE exhaust heat recovery applications, according to the current literature. The most acceptable working fluids for ICE jacket cooling water recovery applications are R123, R245fa, R245ca, and R134a.

The motivation of this work is to improve the comprehensive performance of marine ICE with ORC and utilize the waste heat of the exhaust and the jacket water. In this present work, the validation of the marine ICE is conducted under ICE part-load conditions. the proposed ICE-ORC system is considered with five selected working fluids with low global warming potential and ozone depletion potential parameters. The net output power and thermal efficiency for each of the selected working fluids were obtained.

2. Instructions

In this study, an in-line six-cylinder turbocharged diesel engine is selected. The marine distributed combined cycle system is shown in Figure 1. The ICE in the system is a turbocharged diesel engine with a rated output power of 970kW (in fact, there are two identical ICEs on board). The design fuel of the ICE is diesel the LHV is 42500 kJ/kg. The air enters the cylinder of the ICE after being pressurized and burns with the fuel. The exhaust gas with high-temperature drives the turbine of the turbocharger to increase the pressure of inlet air. The temperature of the exhaust of turbocharger is about 400℃, which is a medium-grade heat source.

Herein, we use ORC to recover the waste energy of exhaust gas and generate additional power (electricity) for the equipment on board, The main components of ORC include an evaporator, expander, condenser, working medium tank, and working medium pump. Besides, the waste energy of exhaust can be recovered by Li-Br absorption refrigerant to provide cold energy for the personnel on board. Additionally, the waste heat of jacket water of ICE can be recovered to produce hot water with a temperature of 80℃.

The exhaust gas after diesel combustion contains nitrogen oxides and sulfides. Considering the low-temperature corrosion of the exhaust gas, the temperature of the flue gas after ORC equipment can be reduced to 160℃. The main parameters of the marine internal combustion engine are shown in Table 1. The main parameters of the ICE under different loads are shown in Table 2. The flow of exhaust rate is calculated by the sum of the mass flow rates of air and fuel. The gas composition of the ICE exhaust gas is given in Table 3.

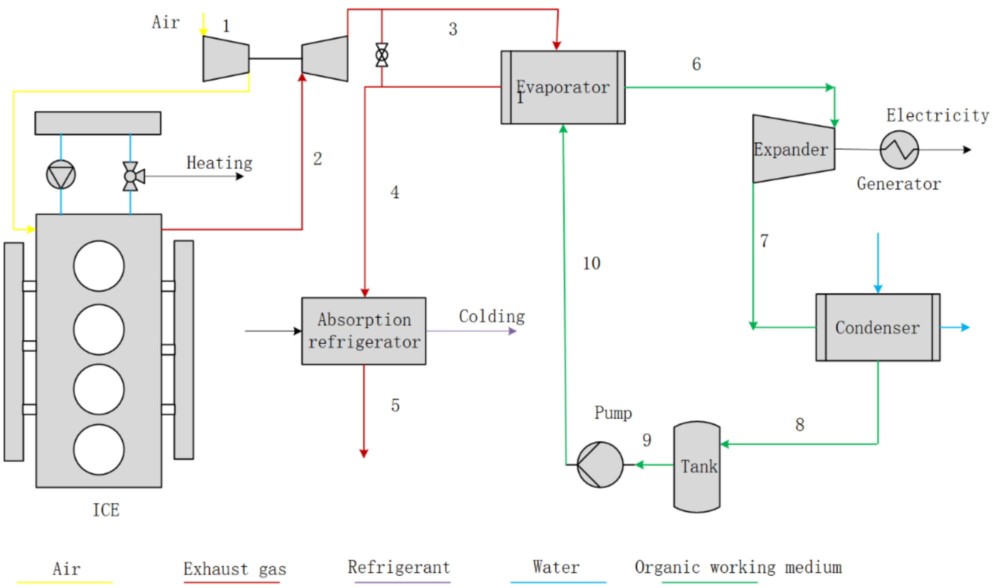

Figure 1. Diagram of the marine mobile distributed system.

Table 1. The main parameters of the ICE [22].

Items	Parameters
Tpye	6320ZCd
Number of cylinders	6
Cylinder diameter	320 mm
Piston stroke	440 mm
Compression ratio	12.6
Maximum power	970 kW
Maximum speed	400 r/min

Table 2. The main parameters of the ICE under different loads [22].

Items	Power loads			Units
	60%	80%	100%	
Power output	606	788	970	kW
Temperature of exhaust gas	220	300	400	℃
Temperature of the exhaust gas before turbo	280	375	480	℃
Mass flow rate of fuel	127.3	165.5	203.7	kg/h
Mass flow rate of air	1.46	1.9	2.34	kg/s
Mass flow rate of exhaust gas	1.5	1.95	2.4	kg/s

Table 3. The composition of ICE exhaust gas.

Composition	Mass fraction
N_2	0.73749
O_2	0.13188
CO_2	0.06507
H_2O	0.05295
Ar	0.01259

3. Mathematical modeling

3.1. Mass and energy equations

The whole system contains three cycles: Diesel engine (Diesel cycle), Li-Br absorption cycle, and ORC. In order to thermodynamically analyze the proposed ICE-ORC system, the conservation equations of mass and energy are used as follows:

Mass equation[23, 24]:

$$\sum \dot{m}_{\mathrm{in}} = \sum \dot{m}_{\mathrm{out}} \tag{1}$$

Energy equation

$$\sum \dot{Q} - \sum \dot{W} = \sum \dot{m}_{\text{out}} h_{\text{out}} - \sum \dot{m}_{\text{in}} h_{\text{in}} \tag{2}$$

3.2. Marine diesel engine prime mover

The thermal energy ($\dot{Q}_{\text{f}}$) supplied by the fuel and the thermal efficiency of the prime mover PM (η_{PM}) can be estimated by:

$$\dot{Q}_{\text{f}} = \dot{m}_{\text{f}} \times LHV_{\text{f}} \tag{3}$$

$$\eta_{\text{PM}} = \frac{\dot{W}_{\text{PM}}}{\dot{Q}_{\text{f}}} \tag{4}$$

The enthalpy of exhaust gas is calculated by:

$$h_{\text{PM}} = \chi_{\text{CO2}} h_{\text{CO2}}(T) + \chi_{\text{O2}} h_{\text{O2}}(T) + \chi_{\text{N2}} h_{\text{N2}}(T) + \chi_{\text{H2O}} h_{\text{H2O}}(T) \tag{5}$$

Where χ_k is the mass fraction of each composition, and $h_k(T)$ is the enthalpy of each component at a specific temperature.

Heat exchangers have been installed to recover the waste heat of the exhaust gas. On one hand, the recovered energy is used by the ORC subsystem to generate electricity, on the other hand, it is used by the Li-Br absorption chiller to produce cool energy. The energy balance of the heat exchanger for ORC can be written as:

$$\dot{Q}_{\text{HE\_E}} = \dot{m}_{\text{PM}} \times (h_3 - h_4) \tag{6}$$

While the recovered energy by the heat exchanger for the absorption chiller ($\dot{Q}_{\text{HE\_A}}$) can be calculated as[24]:

$$\dot{Q}_{\text{HE\_A}} = \dot{m}_{\text{PM}} \times (h_4 - h_5) \tag{7}$$

$$\dot{m}_{\text{PM}} = \dot{m}_3 = \dot{m}_4 = \dot{m}_5 \tag{8}$$

3.3. Organic Rankine cycle

For the ORC subsystem, the recovered waste energy by evaporator ($\dot{Q}_{\text{E}}$) can be calculated by[25]:

$$\dot{Q}_{\text{E}} = \dot{m}_{\text{R}} \times (h_6 - h_{10}) \tag{9}$$

where $\dot{m}_{\text{R}}$ is the mass flow rate of the organic working medium. Additionally, the useful work (electricity) output by the expander is[26, 27]:

$$\dot{W}_{\text{E}} = \dot{m}_{\text{R}} \times (h_6 - h_7) \tag{10}$$

The condenser is used to reduce the organic working medium from gaseous to liquid, the released energy by the condenser ($\dot{Q}_{\mathrm{C}}$) can be calculated by[28]:

$$\dot{Q}_{\mathrm{C}} = \dot{m}_{\mathrm{R}} \times (h_7 - h_8) \tag{11}$$

The consumed energy by the pump ($\dot{W}_{\mathrm{P}}$) is[29]:

$$\dot{W}_{\mathrm{P}} = \dot{m}_{\mathrm{R}} \times (h_{10} - h_9) \tag{12}$$

The net power output of the ORC subsystem is evaluated by[30, 31]:

$$\dot{W}_{\mathrm{ORC}} = \dot{W}_{\mathrm{E}} - \dot{W}_{\mathrm{P}} \tag{13}$$

The isentropic efficiencies of the expander and the pump can be defined as:

$$\eta_{\mathrm{E,s}} = \frac{h_{\mathrm{in}} - h_{\mathrm{out}}}{h_{\mathrm{in}} - h_{\mathrm{s,out}}} \tag{14}$$

$$\eta_{\mathrm{P,s}} = \frac{h_{\mathrm{in}} - h_{\mathrm{s,out}}}{h_{\mathrm{in}} - h_{\mathrm{out}}} \tag{15}$$

where h_{in} and h_{out} are the specific enthalpy at the inlet and outlet of turbines or pumps. $h_{\mathrm{s,out}}$ is the specific enthalpy of the outlet in the isentropic process.

The system thermodynamic performance can be evaluated by the net power output. And the ORC efficiency can be defined as:

$$\eta_{\mathrm{ORC}} = \frac{\dot{W}_{\mathrm{ORC}}}{\dot{Q}_{\mathrm{E}}} = \frac{\dot{W}_{\mathrm{E}} - \dot{W}_{\mathrm{P}}}{\dot{m}_{\mathrm{R}} \times (h_6 - h_{10})} \tag{16}$$

3.4. Overall proposed ICE-ORC system

The total power output and the efficiency of the proposed ICE-ORC system can be estimated by the following equations[32, 33]:

$$\dot{W}_{\mathrm{PM\text{-}ORC}} = \dot{W}_{\mathrm{PM}} + \dot{W}_{\mathrm{ORC}} \tag{17}$$

$$\eta_{\mathrm{PM\text{-}ORC}} = \frac{\dot{W}_{\mathrm{PM\text{-}ORC}}}{\dot{Q}_{\mathrm{f}}} \tag{18}$$

In this proposed ICE-ORC system, the waste energy can be recovered to provide cooling can heating. The produced cool energy of the lithium bromide refrigeration unit can be estimated by the following[34]:

$$\dot{Q}_{\mathrm{cooling}} = \dot{Q}_{\mathrm{re\text{-}heat}} \times COP \tag{19}$$

where, $\dot{Q}_{\mathrm{re\text{-}heat}}$ is the required heat load for driving the refrigeration, COP is the coefficient of performance of the lithium bromide refrigeration.

Additionally, the produced heat energy from the jacked water can be estimated by the following:

$$\dot{Q}_{\text{heating}} = \dot{Q}_{\text{re-jacket}} \times \eta_{\text{HE}} \tag{20}$$

where $\dot{Q}_{\text{re-jacket}}$ is the recovered heat load from the jacked water, η_{HE} is the thermal efficiency of the heat exchangers.

The total useful thermal energy of the proposed ICE-ORC system can be calculated as[1]:

$$\dot{Q}_{\text{ICE-ORC}} = \dot{W}_{\text{PM-ORC}} + \dot{Q}_{\text{cooling}} + \dot{Q}_{\text{heating}} \tag{21}$$

In addition, the total energy utilization efficiency of the proposed ICE-ORC system can be calculated as:

$$\eta_{\text{ICE-ORC}} = \frac{\dot{Q}_{\text{ICE-ORC}}}{\dot{Q}_{\text{f}}} \tag{22}$$

3.5. Model validation

In order to validate the modeling results, it is assumed that:

- All processes take place at a steady state
- The pressure drop due to flow friction is neglected
- The temperature and mass flow rate is constant for the exhaust gas from the ICE.
- The ambient operating temperature and pressure are 15℃ and 1.0 bar, respectively.
- There are no energy losses in the generator.

The viable mathematical model of the ICE system and ORC subsystem is built by Ebsilon® *Professional*, which is widely used in power plant design, evaluation, optimization, and other thermal cycle processes. The screenshot of the process flow diagram is shown in Figure 2. The revoved waste energy is calculated in Excel. In order to validate the accuracy of the simulation process of the proposed model, a series of selected parameters were used to compare the results. It is known from the Table 4. There is little difference between design values and simulation values. The main parameters of the ORC are shown in Table 5. The thermal efficiency of the heat exchangers and the COP of the absorption refrigeration are shown in Table 6.

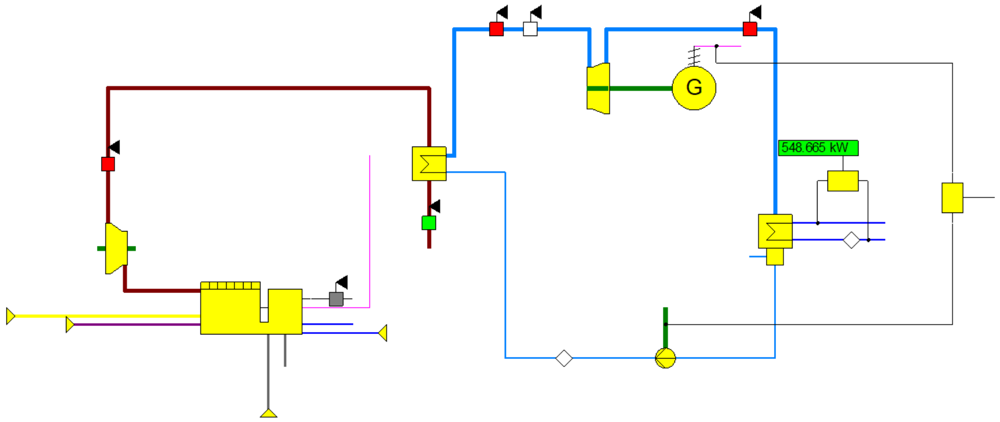

Figure 2. The screenshot of the process flow diagram.

Table 4. The main parameters of the ICE.

Items	Load=60%		Load=100%		Units
	Ref	Sim	Ref	Sim	
Power output	606	606.00	970	970.00	kW
Temperature of exhaust gas	220	219.85	400	401.38	℃
Temperature of exhaust gas before turbo	280	280.00	480	480.00	℃
Mass flow rate of fuel	127.3	126.00	203.7	205.20	kg/h
Mass flow rate of air	1.46	1.465	2.34	2.343	kg/s
Mass flow rate of exhaust gas	1.5	1.500	2.4	2.400	kg/s

Table 5. The main parameters of the ORC.

Items	Parameter
Mechanical efficiency of the turbine	0.95
Isentropic efficiency of the turbine	0.88
Generator efficiency	0.95
Mechanical efficiency of the pump	0.95
Isentropic efficiency of the pump	0.88
The pressure of the outlet of the pump	2.4 MPa

Table 6. The η_{HE} of the heat exchangers and the COP of the absorption refrigeration.

Items	Parameter
η_{HE}	0.8 [35]
COP	0.76 [36]

4. Results and discussion

Organic working fluids with a low global warming potential and ozone depletion potential were selected. Table 7 shows the properties of the five working fluids (R1233zd (E), R1234ze (z), R245fa, butane, and pentane) selected for further simulation.

Additionally, the waste energy recovery performance of the proposed ICE-ORC system under different load conditions (60%, 80%, and 100%) was studied. In order to compare the contribution of different organic working mediums to the proposed system under the same working condition, the temperature of the organic working medium is set as the critical temperature, and the pressure is 2.4MPa.

Table 7. The organic working fluids used in ORC system .

Working fluid	Normal boiling point (℃)	Critical temperature (℃)	Critical pressure (bar)	ODP	GWP
R1233zd(E)	18	166.4	36	0.0003	NA
R1234ze(Z)	9.7	150.1	35	0	6
R245fa	15	154	37	0	1030
Butane	-0.5	151.9	37.9	NA	NA
Pentane	36	196.6	33.6	0	7

The simulation results of different organic working fluids under the power load of 60%, 80%, and 100% are shown in Figure 3.

It can be seen that different organic working fluids have different effects on the ORC subsystem under the same ICE operating conditions. And the butane contributes the highest net output power of 11.84kW (power load of 60%), 37.77kW (power load of 80%), and 78.01kW (power load of 100%) among the five selected organic working fluids. Secondly, R1234ze (z) shows the net output power of 11.47kW (power load of 60%), 35.58kW (power load of 80%), and 75.54kW (power load of 100%).

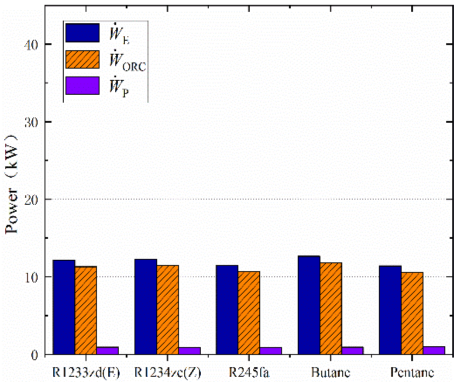

(a) Power load of PM is 60%

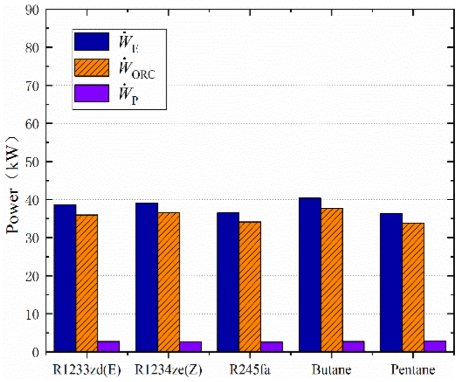

(b) Power load of PM is 80%

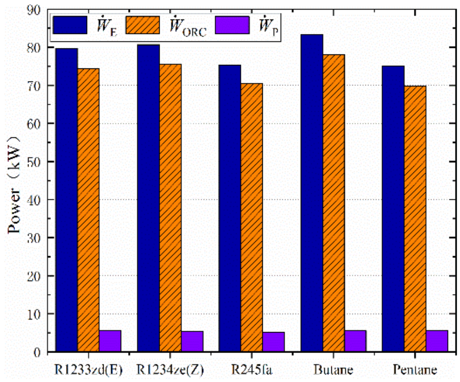

(c) Power load of PM is 100%

Figure 3. Simulation results of different organic working fluids.

The *T-S* characteristics of the ORC system using different organic working fluids are shown in Figure 4. By drawing the *T-S* diagram of the organic working fluid, it is very intuitive to see how much heat various organic working fluids absorb when they do work and the strength of the working fluid can be reflected.

For the convenience of comparison, the length of the entropy value on the abscissa in the figure is 1.6 (kJ/kg·K), and the length of the temperature on the ordinate is 200 (℃). Due to the different characteristics of different organic working fluids, the working ability is also different. The blue curve in the figure is the characteristic curve of the working fluid, and the area enclosed by the characteristic curve is the circulating net heat of the ORC. It can be seen that the Butane (d) shows the area enclosed by the curves in Figure 4 (d) is the largest, indicating that the ORC output work with Butane as the organic working fluid is the largest under the same conditions.

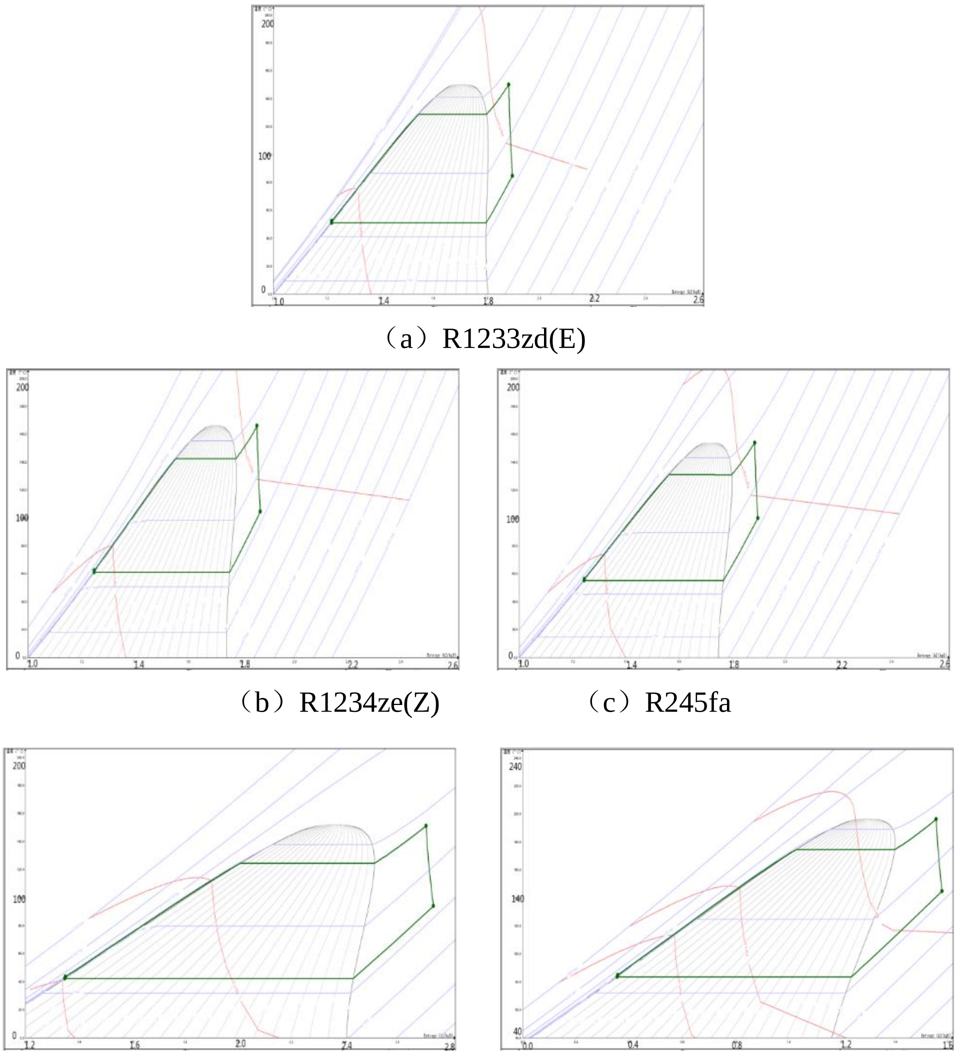

（a）R1233zd(E)

（b）R1234ze(Z)　　（c）R245fa

（d）Butane　　（e）Pentane

Figure 4. The *T-S* diagram of ORC under different organic working fluids.

The ORC efficiency under different organic working fluids is described in Figure 5. It can be seen that the butane shows the highest efficiencies of 12.00% (60%), 12.37% (80%), and 12.27% (100%). While the pentane has the lowest efficiencies under all of the three working loads.

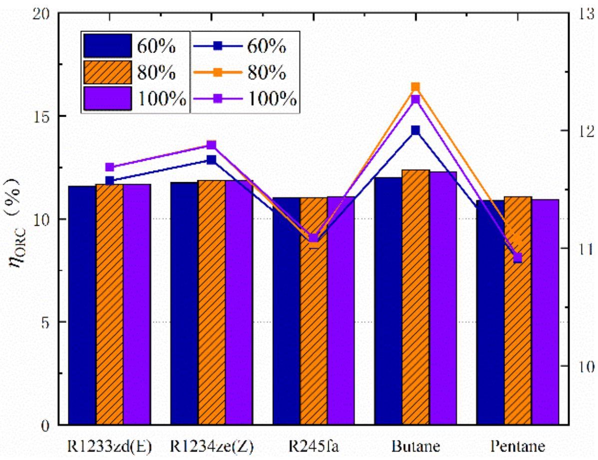

Figure 5. The ORC efficiency under different organic working fluids.

The power outputs of both the proposed ICE-ORC and the conventional ICE are depicted in Figure 6. The quantity of power produced was raised by raising the engine load. Engine exhaust power rose as engine load increased, resulting in enhanced power recovery from the exhaust system. As a result, as engine load grows, bottoming system power output increases. The power output of ICE is 970, while the ICE-ORC is 1044.33kW (R1233zd), 1045.54kW (R1234ze), 1040.51kW (R245fa), 1048.01kW (butane), 1039.77kW (pentane).

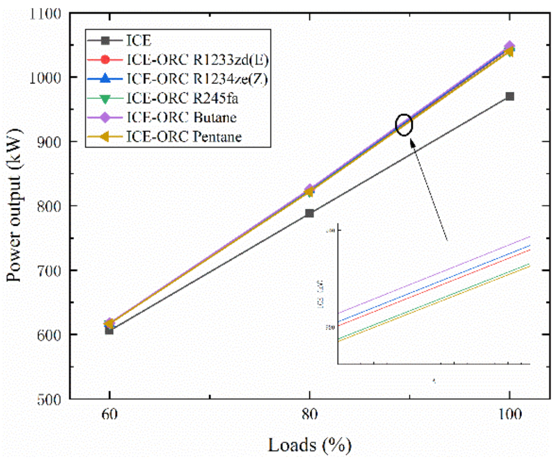

Figure 6. The power output of the proposed ICE-ORC system.

The energy outputs of the proposed ICE-ORC system are shown in Figure 7. By increasing the engine load, the power output of the PM, and the amount of the exhaust gas and jacked water have been increased. In this proposed ICE-ORC system, the waste heat of exhaust gas can be recovered to provide the cool energy via the absorption cycle, while the waste heat of jacked water can be recovered to produce hot water for the people on board. The efficiencies of the proposed ICE-ORC are 70.54%, 69.35%, 67.94% under the PM loads of 60%, 80%, 100%, respectively. I.e., the total thermal efficiency is decreasing with the increase of the PM load. For the reason that the PM efficiency is quite low under lower PM loads, much energy loss can be recovered by the exhaust gas and the jacket water.

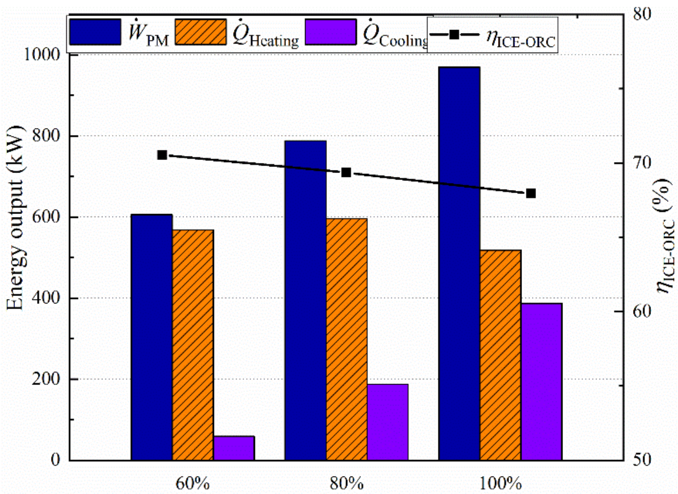

Figure 7. The energy outputs of the proposed ICE-ORC system.

The energy flow diagram of the proposed ICE-ORC system using butane as organic working fluid under full load conditions is shown in Figure 8. It can be seen that the total energy input is 2873.9 kJ, and the power output is 970 kJ. Additionally, the total waste energy of the exhaust gas is 1055.3 kJ, of which the energy effectively recovered by the ORC (Butane) is 78.01 kJ (η_{ORC} =12.27%). Herein, the waste heat of jacket water is recovered to provide heat energy, and the thermal energy recovered is 518 kJ. The total thermal efficiency of the proposed ICE-ORC is 67.94%. The energy used for turbo is 212.9 kJ, because the ICE selected is a turbo charged equipment, and a certain part of waste energy can not be recovered by this part.

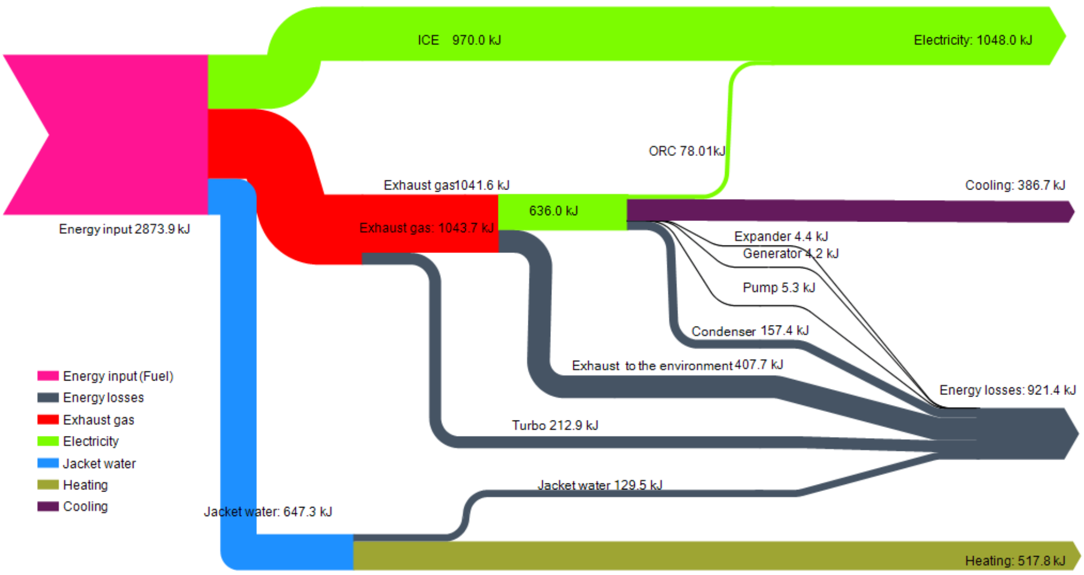

Figure 8. Energy flow diagram of proposed ICE-ORC system.

5. Conclusions

In this paper, an ICE-ORC with cooling, heating and power generation system was developed to analyze the performance of waste heat recovery from the exhaust gas and the jacket water of a heavy-duty marine diesel engine. Five different working fluids with low ODP and GWP were selected to analyze the thermal performance of the proposed ICE-ORC system. The net output power and thermal efficiency for each of the selected working fluids were obtained. The Sankey diagram of the proposed system was employed.

The butane was found to have the best performance among the five selected working fluids. The maximum net power output (1048kW) of the proposed ICE-ORC subsystem was obtained by the working fluids of butane. The power efficiency of the ORC subsystem was 12.27% under the power load of 100%, while the power efficiency of the proposed overall system was 36.47%, which is 2.71% higher than the efficiency of the PM. Besides, the total thermal efficiency was 67.94% when considering the recovered waste energy from the exhaust gas and the jacket water.

Acknowledgment

This study was financially supported by the Ph.D. research startup foundation of Northeast Electric Power University (BSJXM-2020209) and the Fundamental Research Funds for the Central Universities (2018QN035).

Nomenclature and Abbreviations

COP	Coefficient of performance
ICE	Internal combustion engine
LHV_{f}	Lower heating value of fuel, kJ/kg
ORC	Organic Rankine cycle
$\dot{m}_{\mathrm{in}}$	Mass flow rate of inlet, kg/s
$\dot{m}_{\mathrm{out}}$	Mass flow rate of outlet, kg/s
$\dot{m}_{\mathrm{f}}$	Mass flow rate of fuel, kg/s
$\dot{m}_{\mathrm{PM}}$	Mass flow rate of exhaust gas, kg/s
$\dot{m}_{\mathrm{R}}$	Mass flow rate of of the organic working fluid, kg/s
$\dot{Q}_{\mathrm{in}}$	Energy input of the system, kJ/s
$\dot{Q}_{\mathrm{f}}$	Energy supplied by the fuel, kJ/s
$\dot{Q}_{\mathrm{HE\_E}}$	The recovered waste energy by heat exchanger for heating, kJ/s
$\dot{Q}_{\mathrm{HE\_A}}$	The recovered waste energy by heat exchanger for cooling, kJ/s
$\dot{Q}_{\mathrm{E}}$	The recovered waste energy by heat exchanger for ORC, kJ/s
$\dot{Q}_{\mathrm{C}}$	The released energy by the condenser, kJ/s
$\dot{Q}_{\mathrm{re\text{-}heat}}$	The recovered useful energy from exhaust gas, kJ/s
$\dot{Q}_{\mathrm{cooling}}$	The provide cool energy, kJ/s
$\dot{Q}_{\mathrm{re\text{-}jacket}}$	The recovered useful energy from jacket water, kJ/s
$\dot{Q}_{\mathrm{heating}}$	The provide heat energy, kJ/s
$\dot{Q}_{\mathrm{ICE\text{-}ORC}}$	The total useful thermal energy of the ICE-ORC system, kJ/s
$\dot{W}_{\mathrm{out}}$	Power output of the sytem, kJ/s
$\dot{W}_{\mathrm{PM}}$	Power output of the PM, kJ/s
$\dot{W}_{\mathrm{E}}$	Power output of the expander, kJ/s
$\dot{W}_{\mathrm{P}}$	Power consumed by pump, kJ/s
$\dot{W}_{\mathrm{ORC}}$	The net power output of the ORC, kJ/s
$\dot{W}_{\mathrm{PM\text{-}ORC}}$	The power output of the ICE-ORC system, kJ/s
η_{PM}	Thermal efficiency of the PM, %
$\eta_{\mathrm{E,s}}$	The isentropic efficiencies of the expander, %
$\eta_{\mathrm{P,s}}$	The isentropic efficiencies of the pump, %
η_{ORC}	The efficiency of the ORC, %
$\eta_{\mathrm{PM\text{-}ORC}}$	The efficiency of the ICE-ORC system, %
$\eta_{\mathrm{ICE\text{-}ORC}}$	The total thermal efficiency of the ICE-ORC, %
h_{PM}	The enthalpy of exhaust gas, kJ/kg
h_{in}	The specific enthalpy at the inlet, kJ/kg
h_{out}	The specific enthalpy at the outlet, kJ/kg
$h_{\mathrm{s,out}}$	The specific enthalpy of the outlet in the isentropic process, kJ/kg

Appendix A. Calculated thermodynamic parameters of ORC system under 100% load.

Items	H_3(kJ/kg)	H_4(kJ/kg)	T_3(℃)	T_4(℃)	M(kg/s)	W_N(kW)	Eff(%)
R1233zd(E)	520.8	277.1	166.4	62.4	2.61	74.33	11.69
R1234ze(Z)	523.9	267.4	150.2	52.4	2.48	75.54	11.88
R245fa	524.6	275.2	154.5	56.4	2.55	70.51	11.09
Butane	823.9	306.9	151.3	43.6	1.23	78.01	12.27
Pentane	633.8	123	196.9	84.9	1.25	69.77	10.93

Appendix B. Calculated thermodynamic parameters of ORC system under 80% load.

Items	H_3(kJ/kg)	H_4(kJ/kg)	T_3(℃)	T_4(℃)	M(kg/s)	W_N(kW)	Eff(%)
R1233zd(E)	521.5	277.1	166.9	62.4	1.26	35.99	11.69
R1234ze(Z)	524.0	267.4	150.3	52.4	1.20	36.58	11.88
R245fa	524.6	275.2	154.4	56.4	1.24	34.14	11.04
Butane	824.4	306.9	151.5	43.6	0.59	37.77	12.37
Pentane	632.0	123.0	196.3	84.9	0.60	33.80	11.07

Appendix C. Calculated thermodynamic parameters of ORC system under 60% load.

Items	H_3(kJ/kg)	H_4(kJ/kg)	T_3(℃)	T_4(℃)	M(kg/s)	W_N(kW)	Eff(%)
R1233zd(E)	521.0	277.1	166.5	62.4	0.4	11.29	11.57
R1234ze(Z)	524.3	267.4	150.5	52.4	0.38	11.47	11.75
R245fa	524.1	275.2	154.1	56.4	0.39	10.71	11.03
Butane	826.1	306.9	152.1	43.6	0.19	11.84	12.00
Pentane	634.0	123	197	84.9	0.19	10.59	10.91

References

[1] Wang F., *et al.* Design and optimization of hydrogen production by solid oxide electrolyzer with marine engine waste heat recovery and ORC cycle. *Energy Conversion and Management*, 229 (2021), pp. 113775

[2] Feng Y., *et al.* Thermodynamic analysis and performance optimization of the supercritical carbon dioxide Brayton cycle combined with the Kalina cycle for waste heat recovery from a marine low-speed diesel engine. *Energy Conversion and Management*, 206 (2020), pp. 112483

[3] Liu X., *et al.* Performance analysis and optimization of an electricity-cooling cogeneration system for waste heat recovery of marine engine. *Energy Conversion and Management*, 214 (2020), pp. 112887

[4] Kyriakidis F., *et al.* Modeling and optimization of integrated exhaust gas recirculation and multi-stage waste heat recovery in marine engines. *Energy Conversion and Management*, 151 (2017), pp. 286-95

[5] Ouyang T., *et al.* Design and modeling of marine diesel engine multistage waste heat recovery system integrated with flue-gas desulfurization. *Energy Conversion and Management*, 196 (2019), pp. 1353-68

[6] Mondejar M.E., *et al.* A review of the use of organic Rankine cycle power systems for maritime applications. *Renewable and Sustainable Energy Reviews*, 91 (2018), pp. 126-51

[7] Mito M.T., *et al.* Utilizing the scavenge air cooling in improving the performance of marine diesel engine waste heat recovery systems. *Energy*, 142 (2018), pp. 264-76

[8] Mat Nawi Z., *et al.* The potential of exhaust waste heat recovery (WHR) from marine diesel engines via organic rankine cycle. *Energy*, 166 (2019), pp. 17-31

[9] Toro C., *et al.* Analysis and comparison of solar-heat driven Stirling, Brayton and Rankine cycles for space power generation. *Energy*, 120 (2017), pp. 549-64

[10] Lion S., *et al.* Thermodynamic analysis of waste heat recovery using Organic Rankine Cycle (ORC) for a two-stroke low speed marine Diesel engine in IMO Tier II and Tier III operation. *Energy*, 183 (2019), pp. 48-60

[11] Liu X., *et al.* A novel waste heat recovery system combing steam Rankine cycle and organic Rankine cycle for marine engine. *Journal of Cleaner Production*, 265 (2020), pp. 121502

[12] Mohammed A.G., *et al.* Performance analysis of supercritical ORC utilizing marine diesel engine waste heat recovery. *Alexandria Engineering Journal*, 59 (2020), pp. 893-904

[13] Song J., *et al.* Thermodynamic analysis and performance optimization of an Organic Rankine Cycle (ORC) waste heat recovery system for marine diesel engines. *Energy*, 82 (2015), pp. 976-85

[14] Ouyang T., *et al.* Advanced exergo-economic schemes and optimization for medium–low grade waste heat recovery of marine dual-fuel engine integrated with accumulator. *Energy Conversion and Management*, 226 (2020), pp. 113577

[15] Tian H., *et al.* Theoretical research on working fluid selection for a high-temperature regenerative transcritical dual-loop engine organic Rankine cycle. *Energy Conversion and Management*, 86 (2014), pp. 764-73

[16] Shi L., *et al.* A review of modified Organic Rankine cycles (ORCs) for internal combustion engine waste heat recovery (ICE-WHR). *Renewable and Sustainable Energy Reviews*, 92 (2018), pp. 95-110

[17] Orumiyehei A., *et al.* Transient simulation of hybridized system: Waste heat recovery system integrated to ORC and Linear Fresnel collectors from energy and exergy viewpoint. *Renewable Energy*, 185 (2022), pp. 172-86

[18] Nami H., *et al.* Gas turbine exhaust gas heat recovery by organic Rankine cycles (ORC) for offshore combined heat and power applications - Energy and exergy analysis. *Energy*, 165 (2018), pp. 1060-71

[19] Catapano F., *et al.* Development and experimental testing of an integrated prototype based on Stirling, ORC and a latent thermal energy storage system for waste heat recovery in naval application. *Applied Energy*, 311 (2022), pp. 118673

[20] Georgousopoulos S., *et al.* Thermodynamic and techno-economic assessment of pure and zeotropic fluid ORCs for waste heat recovery in a biomass IGCC plant. *Applied Thermal Engineering*, 183 (2021), pp. 116202

[21] Özcan Z., *et al.* A novel working fluid selection and waste heat recovery by an exergoeconomic approach for a geothermally sourced ORC system. *Geothermics*, 95 (2021), pp. 102151

[22] Main technical specifications of diesel engine and its accessories (6320ZCd).

[23] Seyedkavoosi S., *et al.* Exergy-based optimization of an organic Rankine cycle (ORC) for waste heat recovery from an internal combustion engine (ICE). *Applied Thermal Engineering*, 126 (2017), pp. 447-57

[24] Salek F., *et al.* Thermodynamic analysis of diesel engine coupled with ORC and absorption refrigeration cycle. *Energy Conversion and Management*, 140 (2017), pp. 240-6

[25] Wang Z., *et al.* Energy, exergy and economy (3E) investigation of a SOFC-GT-ORC waste heat recovery system for green power ships. *Thermal Science and Engineering Progress*, 32 (2022), pp. 101342

[26] Zhang Y.-F., *et al.* Effect of heat source supplies on system behaviors of ORCs with different capacities: An experimental comparison between the 3 kW and 10 kW unit. *Energy,* 254 (2022), pp. 124267
[27] Zhang T., *et al.* Thermo-economic analysis and optimization of ICE-ORC systems based on a splitter regulation. *Energy,* 226 (2021), pp. 120271
[28] Chatzopoulou M.A., *et al.* Off-design optimisation of organic Rankine cycle (ORC) engines with piston expanders for medium-scale combined heat and power applications. *Applied Energy,* 238 (2019), pp. 1211-36
[29] Yu Z., *et al.* Investigation and optimization of a two-stage cascade ORC system for medium and low-grade waste heat recovery using liquefied natural gas cold energy. *International Journal of Refrigeration,* 135 (2022), pp. 97-112
[30] Chatzopoulou M.A., *et al.* Thermodynamic optimisation of a high-electrical efficiency integrated internal combustion engine – Organic Rankine cycle combined heat and power system. *Applied Energy,* 226 (2018), pp. 1229-51
[31] Song J., *et al.* Parametric optimisation of a combined supercritical CO2 (S-CO2) cycle and organic Rankine cycle (ORC) system for internal combustion engine (ICE) waste-heat recovery. *Energy Conversion and Management,* 218 (2020), pp. 112999
[32] Wang Y., *et al.* Thermodynamic performance comparison between ORC and Kalina cycles for multi-stream waste heat recovery. *Energy Conversion and Management,* 143 (2017), pp. 482-92
[33] Teng S., *et al.* Energy, exergy, economic (3E) analysis, optimization and comparison of different ORC based CHP systems for waste heat recovery. *Case Studies in Thermal Engineering,* 28 (2021), pp. 101444
[34] Lu Z., *et al.* Performance evaluation of a novel CCHP system integrated with MCFC, ISCC and LiBr refrigeration system. *International Journal of Hydrogen Energy,* 47 (2022), pp. 20957-72
[35] Mago P.J., *et al.* Evaluation of a turbine driven CCHP system for large office buildings under different operating strategies. *Energy and Buildings,* 42 (2010), pp. 1628-36
[36] Wang S., *et al.* Thermodynamic and economic analysis of solar assisted CCHP-ORC system with DME as fuel. *Energy Conversion and Management,* 186 (2019), pp. 535-45

Paper submitted: 18.07.2022
Paper revised: 05.09.2022
Paper accepted: 09.09.2022